^{1}H NMR Studies of Plastocyanin from *Scenedesmus obliquus*: Complete Sequence-Specific Assignment, Secondary Structure Analysis, and Global Fold†

Jonathan M. Moore,‡ Walter J. Chazin,‡ Roy Powls,§ and Peter E. Wright*,‡

Department of Molecular Biology, Research Institute of Scripps Clinic, La Jolla, California 92037, and Department of Biochemistry, The University, Liverpool, England L69 3BX

Received March 3, 1988; Revised Manuscript Received May 26, 1988

ABSTRACT: Two-dimensional ^{1}H NMR methods have been used to make sequence-specific resonance assignments for the 97 amino acid residues of the plastocyanin from the green alga *Scenedesmus obliquus*. Assignments were obtained for all backbone protons and the majority of the side-chain protons. Spin system identification relied heavily on the observation of relayed connectivities to the backbone amide proton. Sequence-specific assignments were made by using the sequential assignment procedure. During this process, an extra valine residue was identified that had not been detected in the original amino acid sequence. Elements of regular secondary structure were identified from characteristic NOE connectivities between backbone protons, $^3J_{HN\alpha}$ coupling constant values, and the observation of slowly exchanging amide protons. The protein in solution contains eight β-strands, one short segment of helix, five reverse turns, and five loops. The β-strands may be arranged into two β-sheets on the basis of extensive cross-strand NOE connectivities. The chain-folding topology determined from the NMR experiments is that of a Greek key β-barrel and is similar to that observed for French bean plastocyanin in solution and poplar plastocyanin in the crystalline state. While the overall structures are similar, several differences in local structure between the *S. obliquus* and higher plant plastocyanins have been identified.

Plastocyanin (Pc)[1] is a blue copper protein of molecular weight ~10000 found in higher plants and algae. The protein is an essential component in the photosynthetic electron-transport chain, functioning as a mobile electron carrier between cytochrome *f* and P700 in photosystem I. Plastocyanins are well suited for studies of the mechanisms and pathways of long-range biological electron transfer because they exhibit defined binding sites for other electron-transfer proteins and inorganic reagents (Sykes, 1985; Cookson et al., 1980a,b; Handford et al., 1980).

Amino acid sequences are available for plastocyanins from a number of species, and electron-transfer kinetics for several higher plant and algal proteins have been reported (Sykes, 1985; Jackman et al., 1987; McGinnis et al., 1988). Although there is considerable sequence homology between the plastocyanins from the green and blue-green algae and those from higher plants, there are several important sequence differences that influence the electron-transfer properties. The plastocyanin family thus provides a homologous series of proteins for investigations of the relationship between structure and amino acid sequence and the rates and mechanisms of electron transfer. Although the three-dimensional structure of plastocyanin from a higher plant source (poplar) has been determined to high resolution by X-ray crystallography for both the oxidized (Guss & Freeman, 1983) and reduced (Guss et al., 1986) forms, there is as yet no structural information available for plastocyanins from algal sources. Such structures are needed to allow interpretation of the observed differences in electron-transfer kinetics and active-site pK_a (Jackman et al., 1987; Sinclair-Day et al., 1985). We have thus undertaken NMR experiments to investigate the structure of the plastocyanin from the green alga *Scenedesmus obliquus*. This protein differs substantially in sequence from the poplar Pc for which the structure is known. The most notable changes include deletion of residues *57* and *58*[2] and an unusual exchange of the phenylalanine and tyrosine residues at positions *82* and *83* of the poplar Pc (R. P. Ambler, personal communication). In addition, *S. obliquus* Pc contains a third histidine residue that provides a defined binding site for ruthenium complexes (A. G. Sykes, personal communication) which can be used to probe the mechanism of long-range electron transfer.

The present paper describes spin system identification, sequential resonance assignments, and determination of the global fold of *S. obliquus* plastocyanin. Similar methods have been employed in our laboratory to probe the solution structure and dynamics of French bean plastocyanin (Chazin et al., 1988; Chazin & Wright, 1988). The calculation of solution structures from the NMR data using distance geometry and molecular dynamics methods is reported elsewhere (Moore et al., 1988).

Experimental Procedures

Plastocyanin was isolated from *S. obliquus* and purified as described previously (McGinnis et al., 1988). A single 15-mg sample with A_{278}/A_{597} = 3.5 was used for all experiments. Dialysis and concentration of the protein were performed by using an identical procedure for samples in both ^1H_2O and

† This work was supported by Grant GM36643 from the National Institutes of Health.

‡ Research Institute of Scripps Clinic.

§ University of Liverpool.

[1] Abbreviations: Pc, plastocyanin; NMR, nuclear magnetic resonance; 2D, two-dimensional; COSY, correlated spectroscopy; R-COSY, relayed COSY; DR-COSY, double-relayed COSY; MQ (2Q), multiple-quantum (two-quantum) spectroscopy; MQF-COSY (2QF-COSY), multiple-quantum-filtered (two-quantum-filtered) COSY; TOCSY, total correlation spectroscopy; NOE, nuclear Overhauser effect; NOESY, NOE spectroscopy.

[2] The *S. obliquus* and most higher plant plastocyanins differ in number of amino acid residues. In this paper the higher plant numbering is italicized.

0006-2960/88/0427-7806$01.50/0

^2H_2O. Dialysis was carried out against a 50 mM potassium phosphate buffer, pH 6.2, under argon in an Amicon concentrator equipped with a microvolume accessory. The concentrated solution was then transferred to an NMR tube and reduced with dithionite. The tube was then flushed with argon and sealed with a rubber septum. Samples dissolved in ^1H_2O were brought to a final solvent composition of 90% ^1H_2O/10% ^2H_2O by addition of ^2H_2O. Final samples of Pc were 3–4 mM in protein. pH readings for ^2H_2O solutions were not corrected for isotope effects.

^1H NMR spectra were recorded with Bruker AM-500 and AM-300 spectrometers equipped with Aspect 3000 computers and digital phase-shifting hardware. All two-dimensional NMR experiments were recorded and plotted in the phase-senstitive mode. Time proportional phase incrementation (Bodenhausen et al., 1980; Marion & Wüthrich, 1983) was implemented for quadrature detection in the ω_1 dimension. For all experiments the carrier was placed on the solvent resonance, and 450–700 t_1 experiments were collected, each containing 2048 complex data points. The spectral width in ω_1 was typically set to a value smaller than that in ω_2 in order to maximize digital resolution in the ω_1 dimension. The final data block consisted of 1024 complex points in ω_1 and 2048 complex points in ω_2. Typical values for the digital resolution for experiments at 500 MHz were 2.9 Hz/point in ω_2 and 5.3 Hz/point in ω_1.

For identification of spin systems and sequential assignments, COSY, R-COSY, DR-COSY, 2Q, and NOESY spectra were acquired in ^1H_2O and 2QF-COSY, 2Q, and NOESY spectra were acquired in ^2H_2O. In addition, COSY and NOESY data sets were acquired in ^1H_2O at 288 K to aid in resolving overlapping or degenerate cross-peaks present in the amide fingerprint region of the spectra recorded at higher temperature.

Standard pulse sequences and phase cycling were employed for acquisition of COSY (Marion & Wüthrich, 1983), 2QF-COSY (Rance et al., 1983), NOESY (Bodenhausen et al., 1984), R-COSY (Wagner, 1983), and DR-COSY (Wagner, 1983) spectra. 2Q spectra were acquired by using the pulse sequence and phase-cycling procedure of Braunschweiler et al. (1983), with a composite 180° pulse (Levitt & Freeman, 1979).

Relayed coherence transfer periods in the R-COSY (τ = 40 ms) and DR-COSY (τ_1 = 28 ms, τ_2 = 35 ms) experiments were chosen to optimize coherence transfer from $C^\beta H$ protons to the amide proton, according to calculated transfer efficiencies for a protein with significant β-strand character (Chazin & Wüthrich, 1987).

Data acquired from two-dimensional NMR experiments were processed on an Aspect 3000 data station or a SUN 3/160 workstation equipped with a SKY Warrior array processor. Transform and plotting routines used on the SUN workstation were provided by Dr. Dennis Hare and modified for use on the SUN by Dr. James Sayre. The number of time domain data points used and the relative strength of sine-bell window functions were selected to enhance either sensitivity or resolution. Base-line artifacts (particularly severe for spectra recorded in ^1H_2O solution) were suppressed by application of a pure sine-bell window function or by base-line correction with a spline function following the ω_2 transform. t_1 ridge suppression for cosine-modulated data was implemented by using the method of Otting et al. (1986).

Backbone NH–C^αH vicinal coupling constants were measured from the separation of multiplets for cross-peaks observed in the COSY spectrum recorded in ^1H_2O and transformed with high digital resolution (Marion & Wüthrich, 1983). Cutoffs for large and small coupling constants correspond to $^3J_{HN\alpha} > 8$ Hz and $^3J_{HN\alpha} < 5.5$ Hz, respectively, and are calibrated by using experimental data derived from a globular protein (Pardi et al., 1984). Classification of amide protons as slowly exchanging was made on the basis of observation of persistent NH–C^αH cross-peaks in the 2QF-COSY spectrum recorded less than 24 h after the protein was exchanged into ^2H_2O.

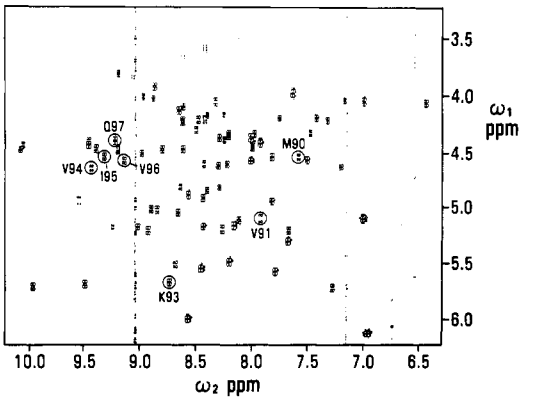

FIGURE 1: NH–C^αH fingerprint region of the COSY spectrum for *S. obliquus* plastocyanin. Numbered peaks are those assigned for residues 90–97, where a sequence error has been shown to exist (see text and Figure 2 legend). (The cross-peaks for Gly 92 are not visible in the spectrum due to bleaching arising from solvent suppression.) The spectrum was recorded in ^1H_2O at pH 6.2 and 303 K.

Results and Discussion

Spin System Identification. Spin system identification for *S. obliquus* plastocyanin was accomplished by using a strategy that relies on the observation of relayed connectivities from side-chain protons to backbone amide protons (Chazin & Wright, 1987). The first step in spin system identification entails examination of the NH–C^αH fingerprint region of the COSY spectrum recorded in ^1H_2O. The amino acid sequence for *S. obliquus* Pc (R. P. Ambler, personal communication) indicates 96 residues, and therefore the fingerprint region should contain cross-peaks for 90 residues (96 residues minus the N-terminal alanine and 5 proline residues). Analysis of the COSY spectrum in ^1H_2O at 303 K (Figure 1) revealed cross-peaks for 85 residues. An additional six NH–C^αH cross-peaks, which were not observed at 303 K due to degeneracy or were bleached as a result of solvent suppression, were observed in the COSY spectrum recorded at 288 K. The one extra NH–C^αH cross-peak was shown, in the course of the sequential assignment procedure, to arise from a residue omitted from the original amino acid sequence (see later).

Delineation of spin systems was performed in several steps. First, identification of glycine spin systems was carried out by observation of the characteristic multiplet structure of the NH–C^αH cross-peaks in the COSY spectrum in ^1H_2O. In addition, unambiguous identification of all 11 glycine spin systems could be made on the basis of observation of remote peaks at $\omega_1 = C^\alpha H + C^{\alpha\prime}H$ at the ω_2 chemical shift of the amide proton in the 2Q spectrum in ^1H_2O. Identification of glycine spin systems with the 2Q experiment is particularly useful in instances when both NH–C^αH cross-peaks do not appear in the COSY spectrum, or, as was observed in the present work, when an NH–C^αH cross-peak is not adequately resolved due to saturation arising from solvent suppression.

The next step in spin system identification requires analysis of the R-COSY and DR-COSY spectra in ^1H_2O such that a maximum number of relayed connectivities from side-chain

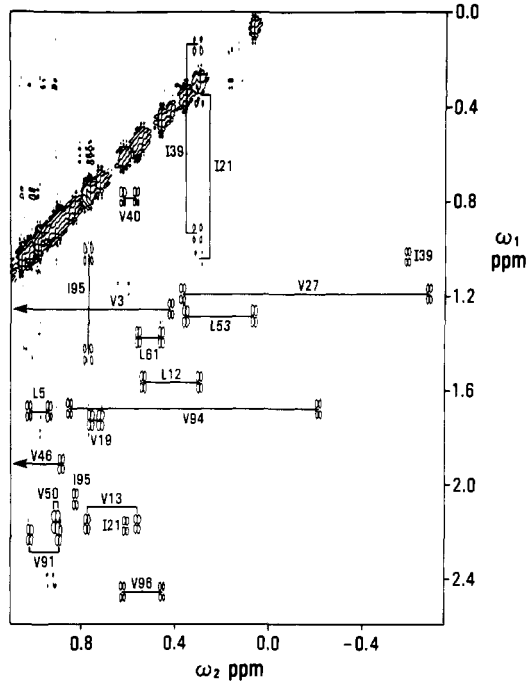

FIGURE 2: High-field methyl region of the 2QF-COSY spectrum of *S. obliquus* plastocyanin. Methyl group cross-peaks from 10 valine, 4 leucine, and 3 isoleucine residues are indicated. The pair of methyl groups corresponding to Val 94 are clearly visible in the spectrum. This residue was not detected in the original amino acid sequence (see text). Single methyl group resonances of Val 3 and Val 46 are located outside the plot limits of the figure. The spectrum was recorded in ^2H_2O at pH 6.2 and 303 K.

protons to backbone amide protons may be obtained (Chazin & Wright, 1987). Complete assignment of spin systems is possible from analysis of R-COSY and DR-COSY spectra for spin systems of the unique type (Gly, Ala, Val, Thr), as well as for the NH–C$^\alpha$H–C$^\beta$H$_2$ fragment of AMX (Ser, Cys, Asp, His, Asn, Phe, Tyr, Trp) and long side chain (Ile, Leu, Met, Glu, Gln, Lys, Arg) spin systems.

Proline spin systems are unique in that the absence of an amide proton makes these spin systems unsuitable for analysis via an amide-proton-based strategy. Identification of proline spin systems, which are usually classified as belonging to the family of long side chain spin systems (Wüthrich, 1983), thus proceeds in a different manner. The partial characterization of these spin systems will be discussed in a separate section.

The COSY spectrum contains 20 of 20 expected methyl group resonances for alanine and threonine residues. Thirteen alanine spin systems could be identified on the basis of NH–C$^\beta$H$_3$ cross-peaks in the R-COSY spectrum in ^1H_2O. In addition, the six threonine spin systems were completely identified by observation of NH–C$^\beta$H and NH–C$^\gamma$H$_3$ relay cross-peaks in the DR-COSY spectrum in ^1H_2O. The remaining alanine C$^\alpha$H–C$^\beta$H$_3$ cross-peak at $\omega_2 = 4.07$, $\omega_1 = 1.29$ was assigned by default to the N-terminal alanine, for which a backbone amide proton resonance is not observed.

From the amino acid composition of *S. obliquus* Pc, one expects to find cross-peaks arising from 10 valine, 4 leucine, and 3 isoleucine residues in the upfield region of the COSY spectrum. This region of the 2QF-COSY spectrum in ^2H_2O is shown in Figure 2. Of the 14 valine/leucine methyl pairs observed, 8 pairs could be identified unambiguously as belonging to valine spin systems on the basis of relayed coherence transfer from both C$^\gamma$H$_3$ groups to the corresponding amide proton resonance in the DR-COSY spectrum in ^1H_2O. The remaining two valine spin systems (Val 46 and Val 13) were identified by the coincidence of the C$^\beta$H chemical shifts in the corresponding C$^\beta$H–C$^\gamma$H$_3$ and NH–C$^\alpha$H–C$^\beta$H spin subsystems. These assignments were corroborated by observation of intraresidue NOE's in the NOESY spectrum (τ = 120 ms) in ^1H_2O.

Two of four leucine spin systems (Leu 55, Leu 12) could be identified on the basis of observed connectivities in the DR-COSY spectrum between both C$^\beta$H protons and the backbone amide proton as well as between both C$^\delta$H$_3$ groups and the same C$^\beta$H protons. The remaining two leucine spin systems could not be identified via relayed connectivities. However, in these cases the C$^\gamma$H–C$^\delta$H$_3$ fragments could be matched with the corresponding backbone NH–C$^\alpha$H–C$^\beta$H$_2$ fragment during sequential assignment via intraresidue NOE's.

Cross-peaks belonging to the three isoleucine spin systems in *S. obliquus* Pc could be readily identified. The six cross-peaks corresponding to C$^\delta$H$_3$–C$^\gamma$H coupling were identified from the unique antiphase triplet coupling pattern of the C$^\delta$H$_3$ (Figure 2). The three C$^\gamma$H$_3$–C$^\beta$H cross-peaks were also easily identified. Two of these isoleucine C$^\gamma$H$_3$ groups could be correlated with a backbone-amide-based spin system via relayed connectivities to the amide proton in the DR-COSY spectrum in ^1H_2O. Correlation of the isoleucine side chain terminal C$^\delta$H$_3$–C$^\gamma$H$_2$ fragment with the NH–C$^\alpha$H–C$^\beta$H–C$^\gamma$H$_3$ fragment was successful for one isoleucine spin system (Ile 39). This spin system was identified by observation of overlapping relayed connectivities from C$^\gamma$H$_3$ to the NH proton as well as from C$^\gamma$H$_3$ to C$^\gamma$H protons in the DR-COSY spectrum. The remaining two isoleucine side chain terminal spin subsystems were matched with the corresponding amide-based spin systems on the basis of intraresidue NOE's. However, since many intraresidue and sequential NOE's were observed for these spin systems, the pairing of spin subsystems was straightforward.

The amino acid composition of *S. obliquus* Pc indicates 32 residues with AMX spin systems and an additional 12 residues, excluding Leu and Ile, that may be classified as long side chain spin systems. Analysis of the R-COSY (τ = 40 ms) and DR-COSY (τ_1 = 28 ms, τ_2 = 35 ms) spectra identified at least one C$^\beta$H proton for 42 of 44 AMX and long side chain spin systems. In addition, the DR-COSY experiment was able to provide connectivities to both C$^\beta$H protons for 28 of 44 such spin systems. Additional C$^\alpha$H–C$^\beta$H connectivities were obtained after careful analysis of the 2QF-COSY and 2Q spectra. In several instances, what was observed as a single cross-peak in the DR-COSY spectrum due to limited resolution in ω_1 could be clearly identified in the 2QF-COSY spectrum as two cross-peaks arising from nearly degenerate C$^\beta$H protons. Also, observation of remote peaks at ω_1 = C$^\beta$H + C$^{\beta'}$H, ω_2 = C$^\alpha$H in the 2Q spectrum was useful for identification and confirmation of C$^\beta$H proton resonances in instances where $^3J_{\alpha\beta}$ is small and relayed coherence transfer is severely attenuated. Using the above combination of techniques, it was possible to assign 85 of a possible 88 C$^\beta$H proton resonances for AMX and long side chain spin systems.

Identification of ring proton spin systems for the three histidine, four tyrosine, five phenylalanine, and the single tryptophan residue was accomplished by using a combination of the 2QF-COSY, R-COSY, and 2Q experiments.

Cross-peaks corresponding to the C$^\epsilon$H–C$^\delta$H coupling of the imidazole ring were observed for all three histidine residues in the 2QF-COSY or 2Q spectra in ^2H_2O. Since scalar connectivities are generally not observed between histidine ring protons and C$^\beta$H protons [however, see Dalvit et al. (1987)], the imidazole ring of histidine residues may be assigned to the appropriate amide-proton-based spin subsystem via intrare-

sidue NOE's between the $C^{\beta}H$ protons and the $C^{\delta}H$ proton. These NOE connectivities were observed for all three histidine residues, although rather weakly for His 85. However, a strong NOE between the $C^{\delta}H$ and $C^{\alpha}H$ protons of His 85 confirmed this assignment.

Three of four tyrosine residues could be identified in a straightforward manner by inspection of the 2QF-COSY spectrum. A fourth set of cross-peaks that appeared severely broadened and were barely resolved in the 2QF-COSY spectrum were later assigned by default to the remaining tyrosine spin system (Tyr 68) after all other aromatic resonances had been assigned. These resonances are most likely exchange broadened due to an intermediate rate of ring flipping on the NMR time scale. Similar broadening of the aromatic resonances was observed for the corresponding tyrosine Tyr *70* of French bean plastocyanin (Chazin et al., 1988).

The complete set of cross-peaks arising from aromatic ring protons could be identified for three of the five phenylalanine residues in *S. obliquus* Pc from the 2QF-COSY spectrum in ^2H_2O. These assignments were confirmed by observation of relay peaks in the R-COSY spectrum (King & Wright, 1983) as well as through analysis of direct and remote peaks in the 2Q spectrum. For one spin system (Phe 14) where the $C^{\epsilon}H$–$C^{\zeta}H$ cross-peak was close to the diagonal, the $C^{\zeta}H$ chemical shift frequency could be calculated from the ω_1 chemical shift of the remote peak in the 2Q spectrum (Dalvit et al., 1986). The remaining Phe spin system could not be completely assigned, as the $C^{\zeta}H$ resonance was not observed in either the 2QF-COSY or 2Q spectrum.

The benzenoid protons of the single tryptophan residue could be assigned in a straightforward manner from the 2QF-COSY and 2Q spectra and the NOESY (τ = 120 ms) spectrum in ^1H_2O. A network of intraresidue NOE's provide assignments for the $C^{\delta}H$ and $N^{\epsilon}H$ and correlate the indole ring with the appropriate backbone-amide-based spin subsystem.

Aromatic ring spin systems of phenylalanine and tyrosine residues were also matched with the appropriate NH–$C^{\alpha}H$–$C^{\beta}H_2$ fragment on the basis of intraresidue NOE's. No intraresidue NOE's between the ring and the NH–$C^{\alpha}H$–$C^{\beta}H_2$ fragment of the severely broadened Tyr 68 were observed in the NOESY spectrum transformed under standard conditions. However, a very high sensitivity transform using weak weighting functions revealed a weak NOE between the Tyr 68 $C^{\delta}H$ protons and a $C^{\beta}H$ proton assigned to residue 68 in the sequential assignment procedure.

Additional assignments for labile side-chain protons of aromatic residues were also made on the basis of intraresidue NOE's. Tyrosine OH proton resonances (singlets) were assigned for two of the four tyrosine residues (78 and 80) from NOE's observed to $C^{\epsilon}H$ and $C^{\delta}H$.

The NOESY spectrum also provided assignments of the methionine $C^{\epsilon}H_3$ group and the exchangeable $N^{\delta}H_2$ and $N^{\epsilon}H_2$ protons of asparagine and glutamine residues, respectively. For these spin systems scalar coupling between side-chain terminal protons and other side-chain protons is not observed.

Assignment of proline spin systems was made by examination of the 2QF-COSY spectrum in ^2H_2O. Since proline $C^{\alpha}H$ resonances occur in a crowded region of the spectrum, identification of these spin systems was deferred until sequential assignments were complete and all other resonances in this region could be identified. The $C^{\alpha}H$–$C^{\beta}H$ region of the 2QF-COSY spectrum was then searched for $C^{\alpha}H$–$C^{\beta}H$ cross-peaks that had not been previously assigned. Ten extra cross-peaks were found in this region. Eight of these cross-peaks arose from connectivities from the $C^{\alpha}H$ to both $C^{\beta}H$ protons for four proline residues, and a single $C^{\alpha}H$–$C^{\beta}H$ connectivity was observed for an additional proline. The remaining cross-peak in this region arose from the $C^{\delta}H/C^{\delta'}H$ connectivity of Pro 84, as was also observed for French bean Pc (Chazin et al., 1988). Analysis of the 2QF-COSY spectrum identified the missing $C^{\beta}H$ resonance for one proline spin system, and the R-COSY spectrum provided $C^{\delta}H$–$C^{\gamma}H$ connectivities for another proline spin system. $C^{\delta}H$ proton resonances were identified for three of five proline spin system, but these could only be assigned to a particular spin system on the basis of sequential NOE's.

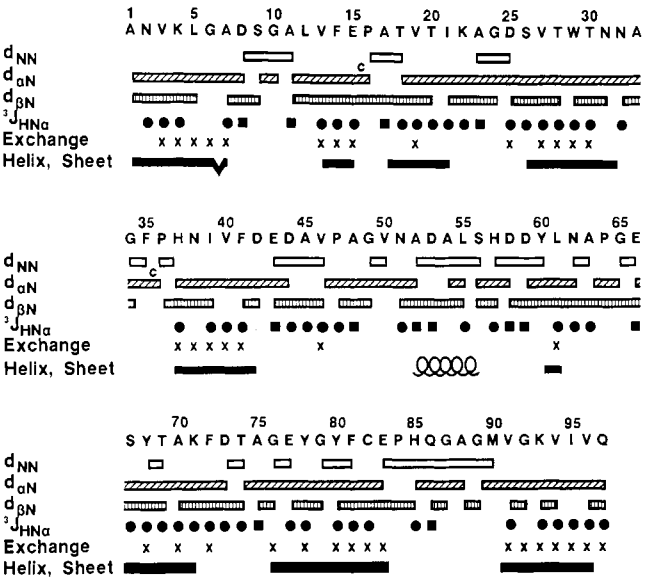

FIGURE 3: Summary of sequential connectivities and additional ^1H NMR data used to characterize secondary structure. The one-letter code for the sequence is given at the top. Characteristic NOE connectivities [$d_{NN}(i,i+1)$; $d_{\alpha N}(i,i+1)$; $d_{\beta N}(i,i+1)$] are indicated by open bars linking the two residues. "c" indicates NOE's involving residue between which there is a cis peptide bond. Values of $^3J_{HN\alpha}$ are classified as small (<5.5 Hz) or large (> 8 Hz) as indicated by boxes and circles, respectively. Backbone amide protons that exchange slowly are indicated with an X. On the bottom line, the locations of β-strands and helix are indicated by filled bars and coils, respectively. The β-bulge is identified by the nick between G6 and S7.

Sequential Resonance Assignments. Sequential resonance assignments for *S. obliquus* plastocyanin were made on the basis of characteristic short proton–proton distances between neighboring residues in NOESY spectra (Billeter et al., 1982). The sequential connectivities observed are shown in Figure 3, and the resonance assignments are summarized in Table I. The shorthand notation of Wüthrich et al. (1984) is used to describe these connectivities. Note that for proline residues $d_{\alpha N}$, d_{NN}, and $d_{\beta N}$ connectivities become $d_{\alpha\delta}$, $d_{N\delta}$, and $d_{\beta\delta}$. *S. obliquus* Pc contains two cis proline residues; the sequential $d_{\alpha\alpha}^{X\text{-Pro}}$ connectivities indicative of the cis peptide bonds are shown in Figure 3 as $d_{\alpha N}$ connectivities labeled "c". NOESY spectra recorded at 303 K (τ = 120 ms) and 288 K (τ = 200 ms) from ^1H_2O solutions were used for the sequential assignments, except for the $d_{\alpha\delta}^{X\text{-Pro}}$ and $d_{\alpha\alpha}^{X\text{-Pro}}$ connectivities that were identified from a NOESY spectrum (τ = 150 ms) in ^2H_2O. A NOESY spectrum recorded in ^1H_2O at lower temperature was useful for resolving chemical shift degeneracies that occur at the higher temperature, as well as for providing NOE connectivities lost at higher temperature due to solvent suppression.

The long stretches of $d_{\alpha N}$ connectivities shown in Figure 3 suggest that a significant portion of the backbone adopts an extended conformation. In addition, the observation of large $^3J_{HN\alpha}$ coupling constants and slowly exchanging NH protons

Table I: ^{1}H NMR Chemical Shifts of *S. obliquus* Plastocyanin (pH 6.2, T = 303 K)

residue	chemical shifts (ppm)					
	NH	$C^{\alpha}H$	$C^{\beta}H$	$C^{\gamma}H$	$C^{\delta}H$	other
Ala 1		4.07	1.29			
Asn 2	8.69	5.46	2.48, 2.635			($N^{\delta}H$) 7.545, 6.94
Val 3	8.80	4.455	1.255	1.14, 0.42		
Lys 4	9.16	4.70	1.895, 1.665			
Leu 5	8.485	4.20	2.52, 1.10	1.69	0.935, 1.025	
Gly 6	7.915	5.075, 3.89				
Ala 7	8.295	4.355	1.43			
Asp 8	9.255	4.12	2.57, 2.71			
Ser 9	7.755	4.175	4.03, 3.86			
Gly 10	8.21	4.32, 3.205				
Ala 11	7.18	4.025	1.22			
Leu 12	8.335	4.04	1.66, 0.90	1.565	0.295, 0.535	
Val 13	7.22	4.62	2.17	0.56, 0.775		
Phe 14	8.85	5.00	2.595, 3.08		6.92	7.22 ($C^{\epsilon}H$), 7.29 ($C^{\zeta}H$)
Glu 15	8.655	5.02	2.03, 1.715			
Pro 16		4.94	2.50, 2.28			
Ala 17	8.40	4.16	1.74			
Thr 18	7.68	5.275	3.875	1.05		
Val 19	8.015	4.56	1.73	0.715, 0.76		
Thr 20	8.205	5.46	3.80	0.98		
Ile 21	9.18	4.71	2.18	1.04, 0.40	0.295	0.61 ($C^{\gamma}H_3$)
Lys 22	8.64	4.79	1.705, 1.78	1.47		
Ala 23	8.52	3.715	1.20			
Gly 24	9.46	4.39, 3.56				
Asp 25	8.29	4.79	2.855, 3.10			
Ser 26	8.455	5.52	3.39, 3.45			
Val 27	8.655	4.115	1.19	−0.68, 0.37		
Thr 28	8.12	5.085	3.71	0.98		
Trp 29	9.95	5.68	3.25, 2.93		6.84	($N^{\epsilon}H$) 9.58, $C^{\eta}H$ 6.975 ($C^{\zeta 2}H$) 6.10, $C^{\zeta 3}H$ 6.86 ($C^{\epsilon 3}H$) 7.81
Thr 30	8.40	4.825	3.74	1.105		
Asn 31	9.245	5.155	2.79			($N^{\delta}H$) 5.105, 6.68
Asn 32	8.915	5.175	3.48, 2.445			($N^{\delta}H$) 7.78, 7.93
Ala 33	8.975	4.47	1.28			
Gly 34	8.765	3.42, 3.54				
Phe 35	5.73	3.19	3.135		6.775	($C^{\zeta}H$) 7.375, ($C^{\epsilon}H$) 7.22
Pro 36		4.97	2.41, 1.48			
His 37	7.285	5.69	2.575, 3.62			($C^{\epsilon}H$) 7.07 ($C^{\delta}H$) 7.72, ($N^{\epsilon}H$) 9.855
Asn 38	10.03	4.47	3.64, 2.64			($N^{\delta}H$) 6.58, 7.97
Ile 39	6.445	4.045	1.03	0.135, 0.94	0.305	−0.59 ($C^{\gamma}H_3$)
Val 40	8.865	3.915	0.77	0.565, 0.62		
Phe 41	8.495	4.295	2.985, 2.64		7.065	($C^{\epsilon}H$) 6.885
Asp 42	8.435	4.575	2.515, 3.05			
Glu 43	8.875	4.015	2.17, 2.13			
Asp 44	8.575	4.86	2.65, 2.855			
Ala 45	8.41	4.73	1.435			
Val 46	7.015	5.075	1.915	0.885, 1.31		
Pro 47		4.28	2.365, 1.555		2.355, 2.675	
Ala 48	8.25	4.145	1.36			
Gly 49	8.62	4.205, 3.62				
Val 50	7.635	3.965	2.16	0.91, 0.91		
Asn 51	8.44	4.885	2.975, 2.745			($N^{\delta}H$) 7.63, 7.09
Ala 52	9.175	3.80	1.42			
Asp 53	8.245	4.375	2.82, 2.72			
Ala 54	7.425	4.18	1.43			
Leu 55	7.00	4.04	1.165, 0.64	1.285	0.065, 0.355	
Ser 56	7.47	4.32	4.10, 3.89			
His 57	9.46	4.415	2.41, 0.93			($C^{\epsilon}H$) 7.05, ($C^{\delta}H$) 8.29
Asp 58	8.635	4.09	2.53			
Asp 59	7.99	4.32	2.13, 2.50			
Tyr 60	8.345	4.59	2.775, 2.96		7.00	($C^{\epsilon}H$) 6.74
Leu 61	9.39	4.455	1.63, 1.24	1.375	0.455, 0.555	
Asn 62	8.385	4.705	2.69			($N^{\delta}H$) 6.72, 7.505
Ala 63	8.22	4.59	1.265			
Pro 64		3.70	2.37, 1.955	1.88, 1.64	3.49, 3.59	
Gly 65	8.43	4.195, 3.575				
Glu 66	7.32	4.20	1.965, 2.07			
Ser 67	8.58	5.965	3.72, 3.68			
Tyr 68	8.90	4.99	2.455, 2.89		7.275	($C^{\epsilon}H$) 7.05
Thr 69	7.79	5.54	3.57	0.905		
Ala 70	8.62	4.46	1.13			
Lys 71	7.82	4.52	1.435, 1.35			

Table I (Continued)

residue	chemical shifts (ppm) NH	$C^{\alpha}H$	$C^{\beta}H$	$C^{\gamma}H$	$C^{\delta}H$	other
Phe 72	8.01	4.355	2.67, 2.37		6.255	($C^{\delta}H$) 7.02, ($C^{\epsilon}H$) 6.495
Asp 73	8.30	4.605	2.49, 2.595			
Thr 74	7.925	4.405	3.88	1.265		
Ala 75	8.97	3.995	1.38			
Gly 76	9.195	4.46, 3.805				
Glu 77	8.165	5.13	1.91, 1.83			
Tyr 78	9.49	5.66	3.635, 3.09		7.155	($C^{\epsilon}H$) 6.66, ($O^{\eta}H$) 10.115
Gly 79	9.54	4.91, 3.93				
Tyr 80	8.44	5.15	1.34, 1.46		6.15	($C^{\epsilon}H$) 5.29, ($O^{\eta}H$) 9.68
Phe 81	9.03	5.15	3.27, 3.04		6.775	($C^{\delta}H$) 7.24, ($C^{\epsilon}H$) 7.025
Cys 82	7.67	5.18	2.805, 3.335			
Glu 83	10.03	4.42	2.36, 2.36			
Pro 84		4.16	0.96, 1.75		5.125, 3.325	
His 85	8.255	5.165	3.78, 3.35			($C^{\delta}H$) 7.14, ($C^{\epsilon}H$) 7.75
Gln 86	8.46	3.97	2.13, 2.53			($N^{\epsilon}H$) 6.05, 6.765
Gly 87	9.065	3.79, 3.875				
Ala 88	7.50	4.55	1.57			
Gly 89	8.01	4.425, 3.77				
Met 90	7.56	4.525	2.15, 1.42			($C^{\epsilon}H_3$) 0.59
Val 91	7.82	4.92	2.215	1.02, 0.895		
Gly 92	8.465	4.79, 2.72				
Lys 93	8.74	5.645	1.805, 1.43			
Val 94	9.435	4.63	1.675	−0.21, 0.85		
Ile 95	9.32	4.52	2.065	1.025, 1.45	0.77	($C^{\gamma}H_3$) 0.825
Val 96	9.14	4.55	2.46	0.62, 0.45		
Gln 97	9.225	4.38	1.945, 2.21			($N^{\epsilon}H$) 6.73, 7.34

for many of these residues implies that the protein possesses significant β-strand character. Identification of these and other elements of regular secondary structure will be discussed in the following section, followed by an analysis of interstrand NOE connectivities that define the packing of the β-strands into the supersecondary structure. The NOE connectivities remaining in the peptide segments indicate several regular reverse turns and loops and are classified accordingly. Finally, on the basis of long-range NOE connectivities, a qualitative assessment of the global fold of the protein in solution is possible.

Polypeptide Segments with Extended Conformation. Polypeptide segments with an extended conformation were identified on the basis of strong $d_{\alpha N}(i,i+1)$ NOE connectivities between adjacent residues. NOESY data are shown for peptide segments 1–8 and 11–15 in parts A and B of Figure 4, respectively. For these peptide segments, strong $d_{\alpha N}(i,i+1)$ connectivities are apparent between all residues except Lys 4/Leu 5. The $C^{\alpha}H$ cross-peak of Lys 4 is not observable at 303 K due to bleaching from solvent saturation. However, a weak $d_{\alpha N}(i,i+1)$ connectivity is present in the spectrum at 288 K (not shown). Observation of a strong $d_{\beta N}(i,i+1)$ connectivity between these residues supports this assignment.

Consecutive $d_{\alpha N}(i,i+1)$ connectivities for sequence positions 18–24, 25–34, 36–43, 47–52, and 56–62 are shown in Figures 5–7. Following the sequence of $d_{\alpha N}(i,i+1)$ and $d_{\beta N}(i,i+1)$ connectivities for these segments was straightforward, with two exceptions. The Ile 21/Lys 22 $d_{\alpha N}(i,i+1)$ connectivity was assigned from the NOESY spectrum acquired at low temperature due to bleaching of the Ile 21 $C^{\alpha}H$ resonance at 303 K. Similarly, the Asp 25/Ser 26 $d_{\alpha N}(i,i+1)$ connectivity, which was rather weak at both temperatures, was confirmed by observation of $d_{\beta N}(i,i+1)$ connectivities from both $C^{\beta}H$ protons of Asp 25 to the amide proton of Ser 26. In addition, a sequential $d_{\alpha\delta}$ connectivity for Val 46/Pro 47 was observed in the NOESY spectrum in ^2H_2O (not shown).

Two long sequences of $d_{\alpha N}(i,i+1)$ connectivities for residues 66–73 and 74–83, separated by a $d_{NN}(i,i+1)$ connectivity between residues Asp 73 and Thr 74, are shown in Figure 8. Proper caution was exercised in the sequential assignment of residues 80–82, as the $C^{\alpha}H$ chemical shifts of Tyr 80 and Phe 81 are nearly degenerate. However, by use of the intraresidue $d_{N\alpha}$ connectivity for Tyr 80 as an internal marker in the NOESY spectrum, slight differences in $C^{\alpha}H$ chemical shift between Tyr 80 and Phe 81 could be resolved and unambiguous assignments could be made. Additional $d_{\beta N}(i,i+1)$ connectivities observed for both $C^{\beta}H$ protons of residues 80 and 81 support these assignments.

A final stretch of $d_{\alpha N}(i,i+1)$ connectivities was observed for residues 90–97, and these are shown in Figure 9. Of particular interest here is a sequence error that was identified during the sequential assignment process. The chemical sequence of *S. obliquus* plastocyanin (R. P. Ambler, personal communication) indicated that the C-terminal region comprising residues 90–96 was Met-Val-Gly-Lys-Ile-Val-Gln. However, in the final stages of sequential assignment, a strong $d_{\alpha N}(i,i+1)$ NOE connectivity was apparent between the $C^{\alpha}H$ proton of a valine spin system and the Ile NH proton. An additional $d_{\alpha N}(i,i+1)$ NOE connectivity was observed from Lys 93 to this valine spin system, placing it between the Lys and Ile residues. Since this valine spin system could be assigned sequentially and its resonances were of normal intensity in both the COSY (see Figures 1 and 2) and NOESY spectra, it clearly does not arise from an impurity. Thus, NMR shows the sequence of residues 90–97 to be Met-Val-Arg-Lys-Val-Ile-Val-Gln. Subsequent resequencing of the C-terminus of *S. obliquus* Pc has confirmed the presence of a valine residue at position 94 (R. P. Ambler, personal communication). The identification of sequence errors during the process of sequential resonance assignment of proteins is not uncommon (Strop et al., 1983; Williamson et al., 1985; Neuhaus et al., 1985; Wagner et al., 1986a; Wemmer et al., 1986).

Helix. NOE connectivities that establish a short stretch of α-helix comprising residues 52–56 are shown in Figure 10. The presence of helical secondary structure in this region is implied by the strong $d_{NN}(i,i+1)$ connectivities observed for these residues and is confirmed by $d_{\alpha N}(i,i+3)$ NOE connectivities between residues 52 and 55 and between residues 53 and 56 and by small $^3J_{HN\alpha}$ coupling constants (<6 Hz) for residues 52–54, and 56. The larger $^3J_{HN\alpha}$ coupling constant

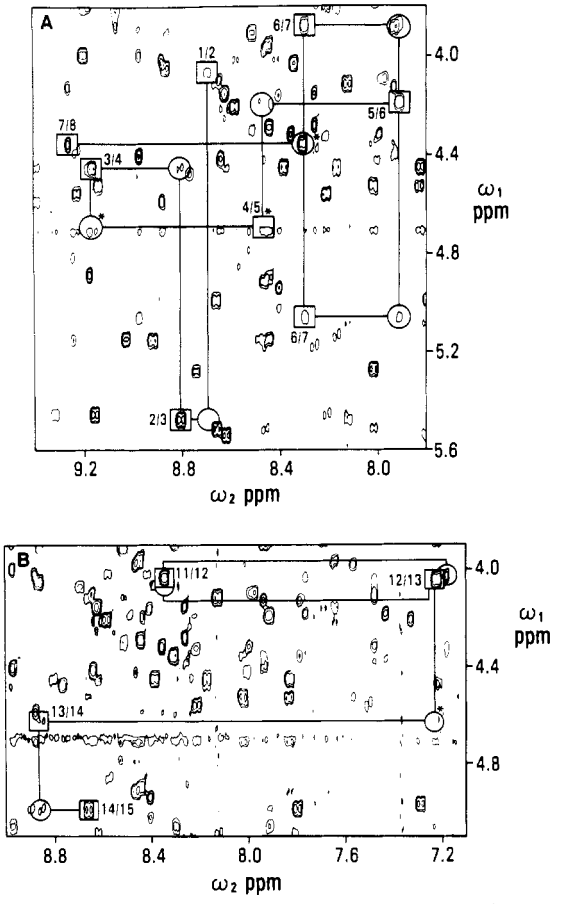

FIGURE 4: Sequential resonance assignments for polypeptide segments in extended conformation. Cross-peaks corresponding to $d_{\alpha N}(i,i+1)$ NOE connectivities are boxed. Circles indicate the position of cross-peaks in the corresponding region of the COSY spectrum acquired under identical experimental conditions. A vertical line is drawn between the COSY cross-peak (circle) and sequential NOE cross-peak (box) for each amide proton resonance. Horizontal lines connect COSY and sequential NOE cross-peaks for each C^{α} proton. The connecting lines provide a guide through the sequential assignment pathway for each polypeptide segment. Asterisks indicate that peaks lying within a box or circle do not arise from the sequential connectivity. The experimental data are shown for (A) A1–D8 and (B) A11–E15. Panels are plotted from a NOESY spectrum (τ_m = 120 ms) acquired in ^1H_2O at pH 6.2 and 303 K. Tracing of sequential connectivities for panel B begins with the $d_{N\alpha}$ connectivity of the initial residue in the polypeptide segment.

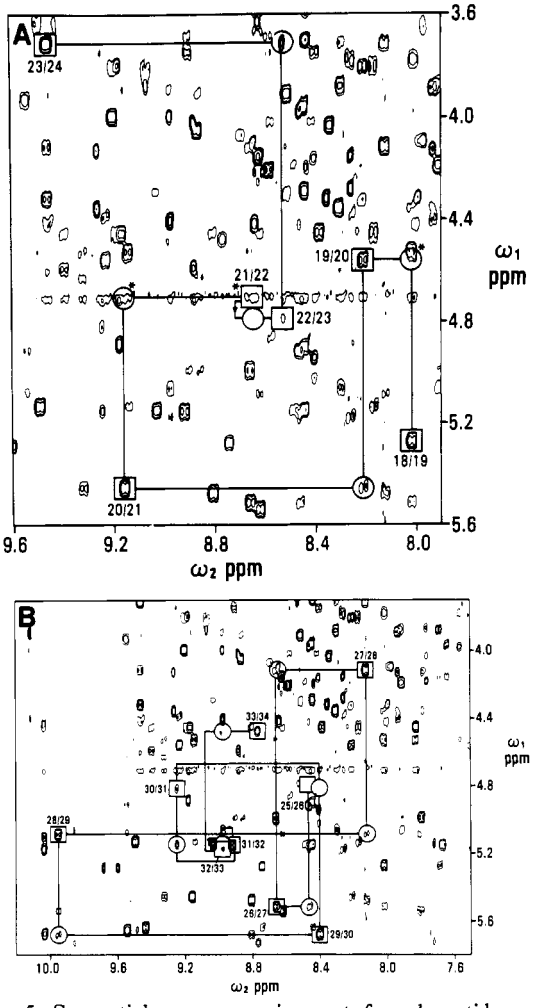

FIGURE 5: Sequential resonance assignments for polypeptide segments in extended conformation. Segments shown are (A) T18–G24 and (B) D25–G34. Symbols used are defined in Figure 4 legend.

(8.6 Hz) observed for residue 55 suggests a possible distortion of the helix at the C-terminal end.

Alignment and Packing of β-Strands. The alignment and packing of β-strands are established on the basis of cross-sheet NOE connectivities between protons on adjacent β-strands. For *S. obliquus* plastocyanin, NOE connectivities characteristic of both parallel and antiparallel packing are observed (Figure 11). The cross-strand distances $d_{\alpha N}(i,j)$ and $d_{NN}(i,j)$ are generally larger than the $d_{\alpha N}(i,i+1)$ and $d_{NN}(i,i+1)$ sequential distances between neighboring residues on the same strand (Wüthrich et al., 1984). Cross-peaks arising due to cross-strand interactions may be distinguished from the sequential type of connectivity by a lower intensity in NOESY spectra. However, the cross-strand $d_{\alpha\alpha}(i,j)$ distance observed in antiparallel β-strands is on the order of 2.3 Å (Wüthrich et al., 1984) and gives rise to NOE's of equal intensity to those of short-range sequential connectivities. The number of interstrand NOE's observed is sufficient to define the packing of β-strands into the two β-sheets shown. The cross-strand $d_{NN}(i,j)$ NOE connectivities between parallel β-strands 18-21/91-96 and 1-6/26-32 are weaker than those observed for the antiparallel β-strands. The types of connectivities and their relative intensities agree well with those predicted for parallel β-strands on the basis of reported X-ray structures (Wüthrich et al., 1984) and are similar to those observed for French bean plastocyanin (Chazin & Wright, 1988). Several expected $d_{\alpha N}(i,j)$ and $d_{NN}(i,j)$ NOE connectivities were not observed due to chemical shift degeneracy or spectral ambiguities arising from resonance overlap. However, the observed coupling constants and the pattern of slowly exchanging amide protons provide strong supporting evidence for the supersecondary structure shown in Figure 11. The short strand containing residues 60 and 61 was included in sheet II of *S. obliquus* Pc by analogy with French bean Pc, for which a complete set of interstrand NOE connectivities was observed (Chazin & Wright, 1988). Its presence in sheet II remains to be confirmed when analysis of structures obtained by distance geometry methods is complete.

Turns and Loops. Criteria for identification and classification of common reverse turns in proteins by NMR methods are well documented (Wüthrich et al., 1984; Wagner et al., 1986b). Identification of turns relies on the observation of characteristic $d_{\alpha N}(i,i+1)$, $d_{NN}(i,i+1)$, and $d_{\alpha N}(i,i+2)$ NOE connectivities between the four amino acid residues comprising the turn. Differentiation between turn types may also be made on the basis of $^3J_{HN\alpha}$ coupling constants for residues at positions 2 and 3 of the turn (Wagner et al., 1986b).

The identification of turns and loops in *S. obliquus* plastocyanin is greatly simplified by previous knowledge of the

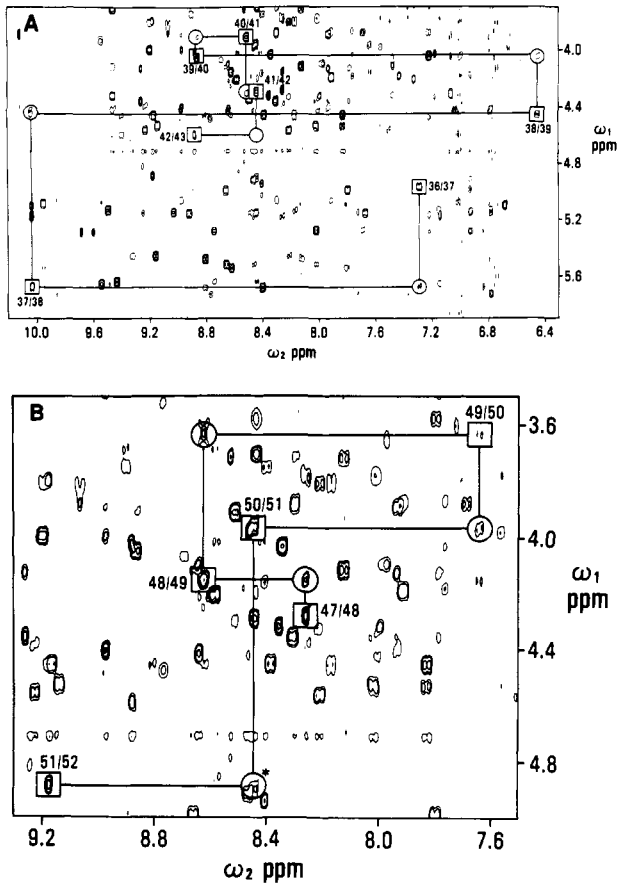

FIGURE 6: Sequential resonance assignments for polypeptide segments in extended conformation. Segments shown are (A) P36–E43 and (B) P47–A52. Symbols used are defined in Figure 4 legend.

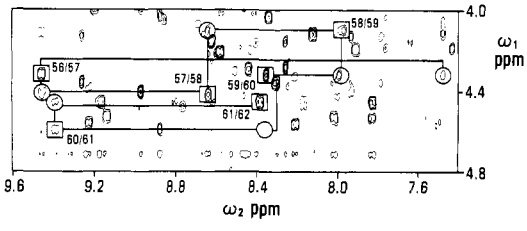

FIGURE 7: Sequential resonance assignments for polypeptide segments in extended conformation. Segment shown is S56–N62. Tracing of sequential connectivities for this panel begins with the $d_{N\alpha}$ connectivity of the initial residue in the polypeptide segment. Symbols used are defined in Figure 4.

strand packing and arrangement of the supersecondary structure. Since the protein consists largely of regular secondary structure, the NOE connectivities in the short peptide segments between β-strands were systematically searched for evidence of regular reverse turns. The reverse turns that could be reliably identified on the basis of both NOE connectivities and $^3J_{HN\alpha}$ coupling constants are summarized in Table II. We note that the NOE connectivities observed for residues 71–74 suggest the presence of a type II′ turn. However, the $^3J_{HN\alpha}$ coupling constant at Phe 72 is much too large (10 Hz), so a regular type II′ turn can be discounted. This emphasizes the importance of using both coupling constants and NOE's to define reverse turns.

Of particular significance in this study is the type VI turn observed for residues 14–17. Such a turn has been observed to occur in plastocyanin from a higher plant source (Chazin et al., 1988) and has been identified here for *S. obliquus* Pc from the strong $d_{\alpha\alpha}(i,i+1)$ NOE connectivity across the cis peptide bond of residues Glu 15 and Pro 16 and a $d_{\alpha N}(i,i+2)$

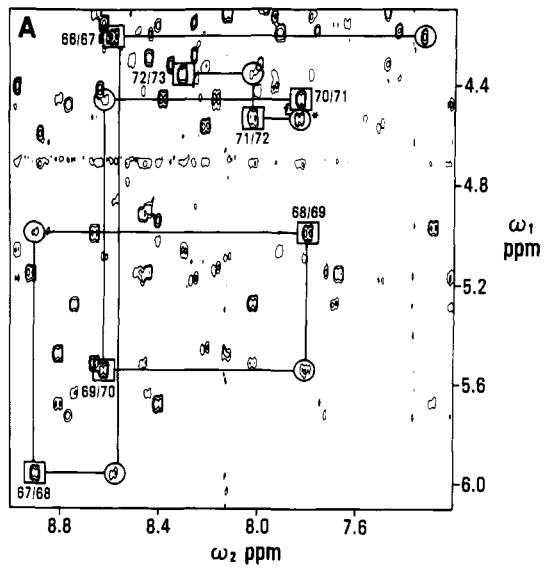

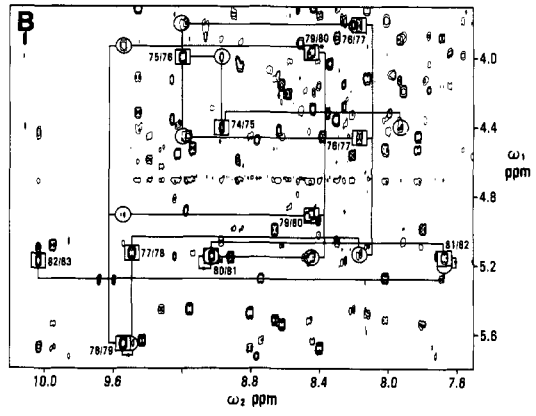

FIGURE 8: Sequential resonance assignments for polypeptide segments in extended conformation. Segments shown are (A) P66–D73 and (B) T74–E83. Tracing of sequential connectivities for panels A and B begins with the $d_{N\alpha}$ connectivity of the initial residue in the polypeptide segment. Symbols used are defined in Figure 4 legend.

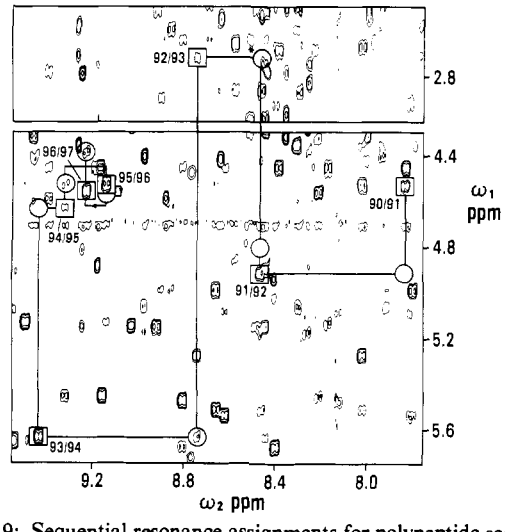

FIGURE 9: Sequential resonance assignments for polypeptide segments in extended conformation. Segment shown is M90–Q97. Symbols used are defined in Figure 4 legend.

connectivity between Glu 15 and Ala 17. This turn may be further classified as a type VIb turn by noting the angular dependence of $^3J_{HN\alpha}$ at position 2. The ϕ_2 dihedral angle for type VI turns is $>-60°$ for type VIa turns and $<-90°$ for type VIb turns (Richardson, 1981). From the angular dependence

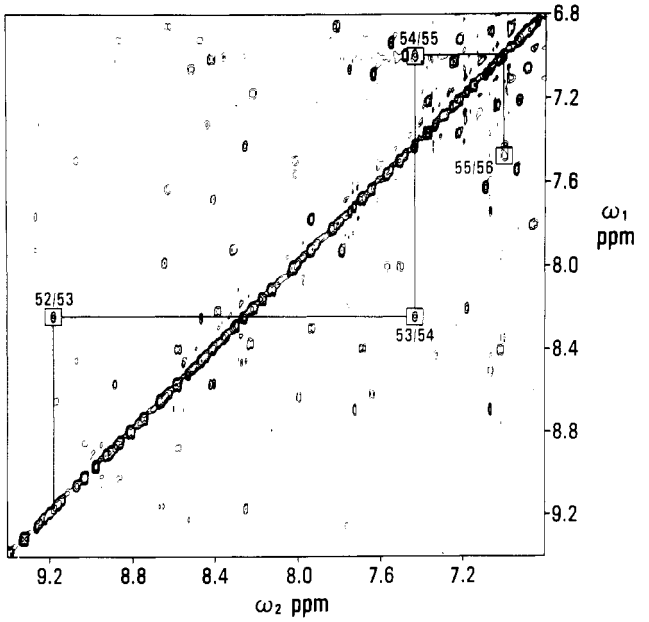

FIGURE 10: Characteristic sequential d_{NN} NOE connectivities for the helical segment A52–S56 from the NOESY spectrum (τ_m = 120 ms) recorded in ^1H_2O at pH 6.2 and 303 K.

of $^3J_{HN\alpha}$ (Pardi et al., 1984), expected values of $^3J_{HN\alpha}$ at position 2 in the turn would be <4 Hz for a type VIa turn and >8 Hz for a type VIb turn. The coupling constant of 10.3 Hz measured from a high-resolution COSY spectrum for residue Glu 15 strongly suggests that this turn falls into the category of type VIb.

A more rigorous classification of turns, especially those for which insufficient experimental evidence is available, will be possible after a thorough analysis of structures generated from the NMR data by distance geometry and molecular dynamics methods is complete. Such work is currently in progress.

Global Fold of S. obliquus Plastocyanin. It is clear from the analysis above that the majority of residues of *S. obliquus* plastocyanin fall in regions of regular secondary structure. Moreover, the constraints imposed by the supersecondary structure (Figure 11) allow a qualitative description of the global fold of the protein in solution. A topology diagram indicating the global fold and packing of *S. obliquus* plastocyanin is shown in Figure 12. The fold is that of a "Greek key" β-barrel (Richardson, 1981) and is similar to that observed for French bean plastocyanin in solution (Chazin & Wright, 1988) and poplar plastocyanin in the crystalline state (Guss & Freeman, 1983). This similarity indicates that the global conformation is conserved in the algal and both higher plant species, which is not surprising considering the 70% sequence homology of *S. obliquus* Pc and 90% sequence homology of French bean Pc relative to the poplar protein. However, several differences in local conformation are observed between the algal and poplar plastocyanins.

The conformation of peptide segment 7–13 appears to differ for *S. obliquus* Pc in solution compared to poplar Pc in the crystalline state. While the poplar protein contains a type I

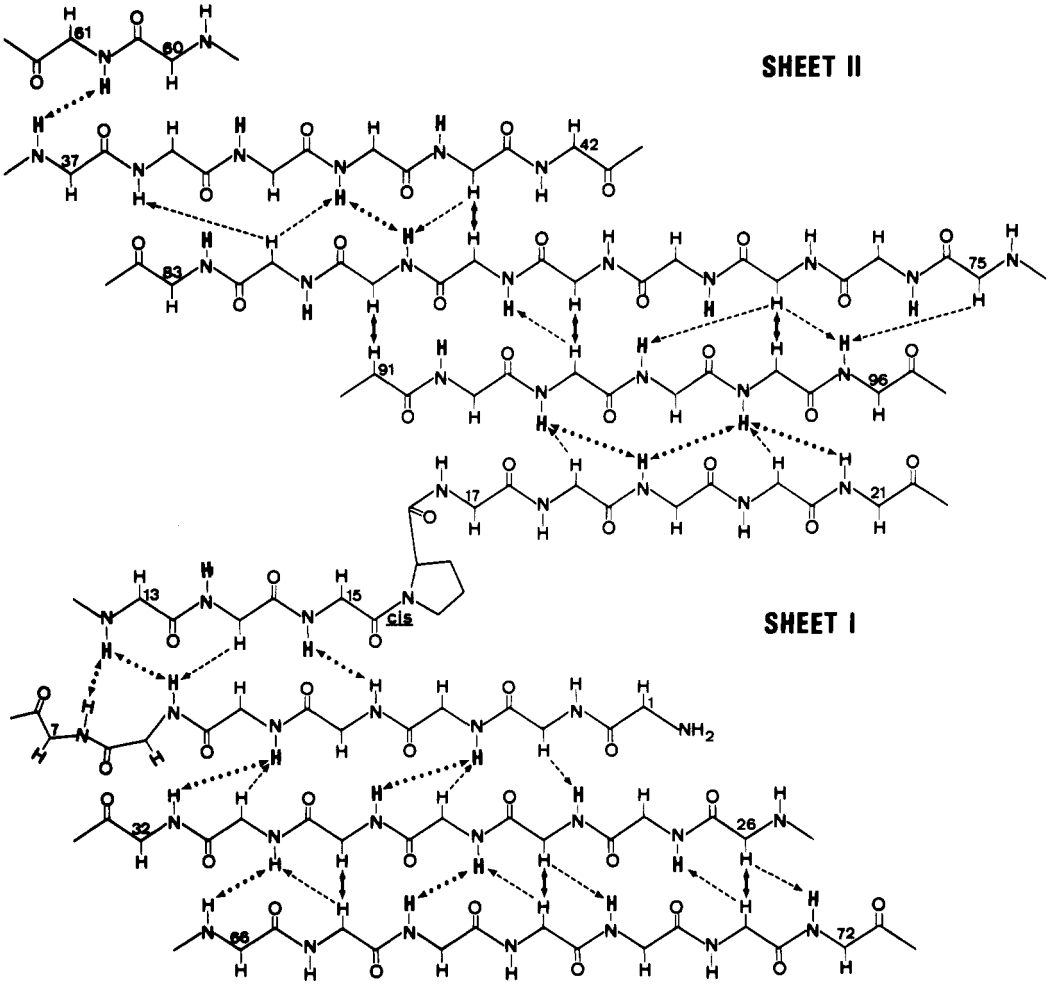

FIGURE 11: Supersecondary structure of *S. obliquus* Cu(I) Pc in solution. The strands within each of the two β-sheets were aligned on the basis of interstrand d_{NN} (<···>), $d_{\alpha N}$ (<---->), and $d_{\alpha\alpha}$ (<—>) NOE connectivities. Residue numbers are given at the beginning and end of each strand.

Table II: Turns and Loops in Plastocyanin

position	*S. obliquus* (NMR) sequence	type[c]	French bean[a] (NMR) sequence	type[c]	poplar[b] (X-ray) sequence	type[c]
7–10	A-D-S-G	L	S-G-D-G	L	A-D-D-G	I
14–17	F-E-P-A	VIb	F-V-P-S	VIb	F-V-P-S	VIb
22–25	K-A-G-D	II or HT	P-S-G-E	II	S-P-G-E	II
32–35	N-A-G-F	L	N-A-G-F	II or HT	N-A-G-F	L
42–45	D-E-D-A	I	D-E-D-E	I	D-E-D-S	I
47–50	P-A-G-V	II or HT	P-A-G-V	II or HT	P-S-G-V	II
58–61[d]	*-*-D-D	no turn[e]	P-E-E-E	II	S-E-E-D	I
65–68[d]	A-P-G-E	II or HT	A-P-G-E	II	A-K-G-E	II
73–76[d]	K-F-D-T	L	T-L-D-T	L	A-L-S-N	L
84–87[d]	C-E-P-H	L	C-S-P-H	L	C-S-P-H	I
88–91[d]	Q-G-A-G	L	Q-G-A-G	I	Q-G-A-G	I

[a] Chazin and Wright (1988). [b] Guss and Freeman (1983). [c] Abbreviations for turn types: L, loop; I, type I; II, type II; VIb, type VIb; HT, half-turn. [d] Higher plant sequence numbering is used for these residues. [e] No turn is observed for these residues due to the deletions at positions 57 and 58.

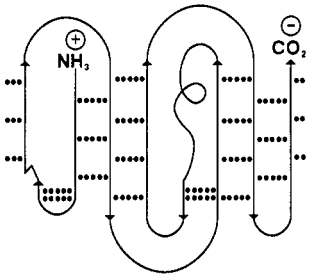

FIGURE 12: Two-dimensional chain-folding topology diagram for *S. obliquus* Cu(I) Pc in solution derived from the NMR data. The chain-folding topology is that of a Greek key β-barrel (Richardson, 1981).

turn at residues *7–10*, no $d_{\alpha N}(i,i+2)$ NOE connectivity was observed for the algal plastocyanin, suggesting a loop or at best an irregular type I turn in this region. In all other regular turns, the $d_{\alpha N}(i,i+2)$ NOE was observed. In addition, the NMR data suggest a β-bulge at residues 6–7 that is not observed for the poplar Pc. NOE's from the NH protons of Gly 6 and Ala 7 to the NH proton of Val 13 provide strong evidence that the Ala 7 amide proton is twisted to the same side of the strand as the Gly 6 amide proton. This backbone conformation would bring the carbonyl oxygen of Ala 7 within hydrogen-bonding distance of the Val 13 amide proton, thus explaining its slow exchange rate. The same set of NOE connectivities characteristic of a β-bulge is observed for French bean Pc (Chazin & Wright, 1988). Other major differences occur between residues 51 and 61 and arise as a direct consequence of the deletion of residues *57* and *58* of poplar Pc from the algal protein. The X-ray structure of poplar plastocyanin contains a short helical segment from residue *51* to *56*, a type I reverse turn at residues *58–61*, and a short stretch of β-strand from position *62* to *64*. The NOE connectivities observed for *S. obliquus* Pc indicate that the helix extends from residue 52 to 56 and is thus one residue shorter than in the poplar Pc. A short β-strand is observed between residues 60 and 62 of *S. obliquus* Pc, corresponding to residues *62–64* of the poplar protein. Thus, the major difference occurs at residues 57–59, where the β-turn found in poplar Pc is eliminated from the algal protein by the deletions.

The assignments, secondary structure analysis, and global fold discussed herein provide a basis for the detailed examination of *S. obliquus* plastocyanin structure and dynamics by NMR, distance geometry, and molecular dynamics methods. Preliminary work in this area has indicated that a high-quality set of solution structures may be generated with NMR distance, dihedral angle, and hydrogen-bonding constraints derived from these data (Moore et al., 1988).

ACKNOWLEDGMENTS

We thank Drs. R. P. Ambler and A. G. Sykes for helpful discussions, L. Tennant for technical assistance, and L. Harvey for preparation of the manuscript.

REFERENCES

Billeter, M., Braun, W., & Wüthrich, K. (1982) *J. Mol. Biol. 155*, 321–346.

Bodenhausen, G., Vold, R. L., & Vold, R. R. (1980) *J. Magn. Reson. 37*, 93–106.

Bodenhausen, G., Kogler, H., & Ernst, R. R. (1984) *J. Magn. Reson. 58*, 370–388.

Braunschweiler, L., Bodenhausen, G., & Ernst, R. R. (1983) *Mol. Phys. 48*, *535*–560.

Chazin, W. J., & Wright, P. E. (1987) *Biopolymers 26*, 973–977.

Chazin, W. J., & Wüthrich, K. (1987) *J. Magn. Reson. 72*, 358–363.

Chazin, W. J., & Wright, P. E. (1988) *J. Mol. Biol. 202*, 623–636.

Chazin, W. J., Rance, M., & Wright, P. E. (1988) *J. Mol. Biol. 202*, 603–622.

Cookson, D. J., Hayes, M. T., & Wright, P. E. (1980a) *Biochim. Biophys. Acta 591*, 162–176.

Cookson, D. J., Hayes, M. T., & Wright, P. E. (1980b) *Nature (London) 283*, 682–683.

Dalvit, C., Rance, M., & Wright, P. E. (1986) *J. Magn. Reson. 69*, 356–361.

Dalvit, C., Wright, P. E., & Rance, M. (1987) *J. Magn. Reson. 71*, 539–543.

Guss, J. M., & Freeman, H. C. (1983) *J. Mol. Biol. 169*, 521–563.

Guss, J. M., Harrowell, P. R., Murata, M., Norris, V. A., & Freeman, H. C. (1986) *J. Mol. Biol. 192*, 361–387.

Handford, P. M., Hill, H. A. O., Lee, W.-K., Henderson, R. A., & Sykes, A. G. (1980) *J. Inorg. Biochem. 13*, 83–88.

Jackman, M. P., Sinclair-Day, J. D., Sisley, M. J., Sykes, A. G., Denys, L. A., & Wright, P. E. (1987) *J. Am. Chem. Soc. 109*, 6443–6449.

King, G. C., & Wright, P. E. (1983) *J. Magn. Reson. 54*, 328–332.

Levitt, M., & Freeman, R. (1979) *J. Magn. Reson. 33*, 473–476.

Marion, D., & Wüthrich, K. (1983) *Biochem. Biophys. Res. Commun. 113*, 967–974.

McGinnis, J., Sinclair-Day, J. D., Sykes, A. G., Powls, R., Moore, J. M., & Wright, P. E. (1988) *Inorg. Chem. 27*, 2306–2312.

Moore, J. M., Case, D. A., Chazin, W. J., Gippert, G. P., Havel, T. A., Powls, R., & Wright, P. E. (1988) *Science*

(Washington, D.C.) 240, 314-317.
Neuhaus, D., Wagner, G., Vašak, M., Kägi, J. H. R., & Wüthrich, K. (1985) Eur. J. Biochem. 151, 257-273.
Otting, G., Widmer, H., Wagner, G., & Wüthrich, K. (1986) J. Magn. Reson. 66, 187-193.
Pardi, A., Billeter, M., & Wüthrich, K. (1984) J. Mol. Biol. 180, 741-751.
Rance, M., Sørensen, O. W., Bodenhausen, G., Wagner, G., Ernst, R. R., & Wüthrich, K. (1983) Biochem. Biophys. Res. Commun. 117, 479-485.
Richardson, J. S. (1981) Adv. Protein Chem. 34, 167-339.
Sinclair-Day, J. D., Sisley, M. J., Sykes, A. G., King, G. C., & Wright, P. E. (1985) J. Chem. Soc., Chem. Commun., 505-507.
Strop, P., Wider, G., & Wüthrich, K. (1983) J. Mol. Biol. 166, 641-667.
Sykes, A. G. (1985) Chem. Soc. Rev. 14, 283-315.
Wagner, G. (1983) J. Magn. Reson. 55, 151-156.
Wagner, G., Neuhaus, D., Wörgötter, E., Vašak, M., Kägi, J. H. R., & Wüthrich, K. (1986a) Eur. J. Biochem. 157, 275-289.
Wagner, G., Neuhaus, D., Wörgötter, E., Vašak, M., Kägi, J. H. R., & Wüthrich, K. (1986b) J. Mol. Biol. 187, 131-135.
Wemmer, D. E., Kumar, N. V., Metrione, R. M., Lazdunski, M., Drobny, G., & Kallenbach, N. R. (1986) Biochemistry 25, 6842-6849.
Williamson, M. P., Havel, T. F., & Wüthrich, K. (1985) J. Mol. Biol. 182, 295-315.
Wüthrich, K. (1983) Biopolymers 22, 131-138.
Wüthrich, K., Billeter, M., & Braun, W. (1984) J. Mol. Biol. 180, 715-740.

Optically Detected Magnetic Resonance Study of Tyrosine Residues in Point-Mutated Bacteriophage T4 Lysozyme†

Sanjib Ghosh, Li-Hsin Zang, and August H. Maki*
Department of Chemistry, University of California, Davis, California 95616
Received May 6, 1988; Revised Manuscript Received June 17, 1988

ABSTRACT: Two spectroscopically distinct types of tyrosine (Tyr) residues in triply point mutated bacteriophage T4 lysozyme, which contains no tryptophan (Trp), have been detected by optical detection of triplet-state magnetic resonance (ODMR) spectroscopy. Their triplet states are characterized by similar E but different D values. The Tyr site which exhibits the lower D value and has the red-shifted phosphorescence origin is quenched by energy transfer to Trp and has D and E values comparable to previously studied Tyr residues. The blue-shifted Tyr site, which is not quenched by Trp, exhibits a larger D value than has been found previously. Calculation of energy-transfer efficiencies of Tyr–Trp pairs based on the crystal structure of the native enzyme provides a possible assignment of Tyr sites to the two different spectral types.

Phosphorescence studies of Tyr residues reveal that their microenvironments in proteins cannot be resolved because of the broad spectra (Longworth, 1971). The zero-field splittings (ZFS)[1] of the lowest triplet states of the tyrosinate anion, the CH_3Hg–tyrosine complex, and Tyr itself have been measured by ODMR spectroscopy (Co et al., 1974; Hershberger & Maki, 1980; Zuclich et al., 1973). However, ODMR study of Tyr in proteins has been reported only in bacterial blue copper azurin, where a single set of ZFS parameters was obtained for the two Tyr residues (Ugurbil et al., 1977a).

Wild-type bacteriophage T4 lysozyme (T4 lysozyme) contains three Trp residues at positions 126, 138, and 158 and six Tyr residues at positions 18, 24, 25, 88, 139, and 161. Triplet-state properties of Trp residues in T4 lysozyme and its various point mutants in which one or two of the Trp residues are substituted by Tyr residues, respectively, have been investigated by low-temperature phosphorescence and ODMR spectroscopy (Ghosh et al., 1988). In this paper, we report our measurements on the triplet state of Tyr residues in wild-type T4 lysozyme and in some mutants, including the one containing nine Tyr residues but no Trp. We have been able to detect two sets of ODMR transitions from this mutant, providing the first example of the recognition of distinct Tyr environments using ODMR. However, the disappearance of the signals of one of the Tyr sites from the native enzyme and from most of the mutants containing Trp residues suggests that the phosphorescence originating from this Tyr residue is selectively quenched by energy transfer to Trp. (For simplicity of terminology, we will refer to a spectroscopically distinct group of residues in the singular, even though the group may contain more than one residue.) On the other hand, the other Tyr residue is not quenched by Trp. The unquenched residue has an unusually high D value. Comparison of the phosphorescence spectra shows that the origin of the quenched Tyr is red-shifted relative to that of the unquenched one.

Materials and Methods

T4 lysozyme and various mutants were generous gifts from L. McIntosh, Institute of Molecular Biology, Eugene, OR. In our description of the protein, the Trp residues are represented by W and Tyr by Y. Thus, WWW = Trp-126, Trp-138, and Trp-158 (wild type), while YYY = Tyr-126, Tyr-138, and Tyr-158 (non-Trp-containing mutant). The other mutants used in this study, which are missing some of the Trp residues,

† This work has been supported by a grant from the National Science Foundation (CHE 85-08752).
* Author to whom correspondence should be addressed.

[1] Abbreviations: D and E, triplet-state zero-field splitting parameters; DTT, dithiothreitol; ODMR, optical detection of triplet-state magnetic resonance; ZFS, zero-field splitting(s).

0006-2960/88/0427-7816$01.50/0